Optik 127 (2016) 4123–4126

Contents lists available at ScienceDirect

Optik

journal homepage: www.elsevier.de/ijleo

Structural and optical properties of Nd^{3+} doped columbite $SrNb_2O_6$

Mete Kaan Ekmekçi[a,*], Murat Erdem[b], Ali Sadi Başak[a,*], Özkan Daniş[a]

[a] Marmara University, Department of Chemistry, Kadıkoy, Istanbul, 34777, Turkey
[b] Marmara University, Department of Physics, Kadıkoy, Istanbul, 34777, Turkey

ARTICLE INFO

Article history:
Received 25 November 2015
Accepted 12 January 2016

Keywords:
Columbite niobates
Molten salt synthesis
Luminescence

ABSTRACT

Nd-doped $SrNb_2O_6$ particles have been prepared by a molten salt method using strontium nitrate, niobium oxide and NaCl–KCl salt mixture as a flux at a relatively low temperature as compared to solid-state reaction method. X-ray diffraction patterns of the pure $SrNb_2O_6$ samples exhibited a single orthorhombic phase. Photoluminescence (PL) properties of Nd-doped samples in near-infrared spectral region were studied in detail. A characteristic luminescence of Nd^{3+} at 1.06 μm was observed for Nd-doped $SrNb_2O_6$. Concentration quenching phenomenon was detected depending on the Nd-doping concentrations at room temperature. This characteristic of the doped samples may be ascribed to the energy transfer between Nd^{3+} and niobate groups (NbO_6).

© 2016 Elsevier GmbH. All rights reserved.

1. Introduction

High purity, compositionally uniform, single phase, small and uniform particle size powders are required for high resolution and high luminous efficiency of the optical materials in photonic device developments. Moreover, it should be pointed out that the selection of host lattices and active centers for such an optical material is important.

The columbite niobates MNb_2O_6 (M = Co, Cd, Ni, Mg, Cu, Zn, and Mn) having orthorhombic unit cell and space group *Pbcn* (60) [1] are known as interesting photoactive host materials due to their high refractive index (for $CaNb_2O_6$, n = 2.07–2.2) and, chemical stability [2].

The structure of MNb_2O_6 columbite consists of two kinds of octahedra as MO_6 and NbO_6. These two octahedras constitute independent repeating zig–zag chains by sharing edges and the chains are connected by sharing corners to form columbite structure [3].

The previous studies have proved that many kinds of rare earth ions can substitute metal ions of columbite structure which consists both MO_6 (M = Metal) and NbO_6 octahedra and do not change the typical orthorombic structure and space group of columbite. Moreover, the columbite host matrix activated with the rare earth (RE^{3+}:Tb^{3+}, Eu^{3+}, Dy^{3+}, Yb^{3+}, Tm^{3+}, Nd^{3+}, Er^{3+}, Pr^{3+}) ions makes a promising candidate for red emission phosphor and, laser material in photonic applications [4–10].

In the columbite structure, such ion substitution requires the calcinations at high temperature to achieve the thermal diffusion of rare earth ions to the metal-oxygen or niobium-oxygen sites of columbite, leading to the enhanced luminescence of trivalent rare earth ions [11].

The molten salt method provides a low-temperature heat treatment process, and gives better chemical homogeneity and finer particles together with better control of particle morphology than those produced by the solid-state reaction [12]. These features make the molten salt process a promising method since it results in improved sinterability [13–15].

In the present study, it was aimed to produce neodymium (Nd^{3+}) doped strontium niobate ceramics by the molten salt technique and investigate into structural and luminescence properties in order to explore its potential application in photonic devices. To our knowledge this is the first report on structural and spectroscopic characterization of strontium niobate ceramic activated with Nd^{3+} using molten salt synthesis.

2. Experimental

Undoped and doped $SrNb_2O_6$ columbite ceramic powders were synthesized via molten salt route by mixing starting materials of strontium nitrate ($Sr(NO_3)_2$) and niobium oxide (Nb_2O_5) at a salt to oxide weight ratio of 6:1. NaCl–KCl salt mixture was used at molar ratio of 1/1. After mixing starting materials (strontium nitrate, niobium oxide and neodymium oxide) in an agate mortar and NaCl and KCl in another mortar, they were mixed well to provide homogeneity. After calcining sufficient amount of mixture at 700 °C for 4 h in an alumina crucible, they were washed with ultra pure water

* Corresponding authors. Tel.: +90 2163479641; fax: +90 2163878783.
E-mail addresses: mekmekci@marmara.edu.tr (M.K. Ekmekçi), asbasak@marmara.edu.tr (A.S. Başak).

http://dx.doi.org/10.1016/j.ijleo.2016.01.107
0030-4026/© 2016 Elsevier GmbH. All rights reserved.

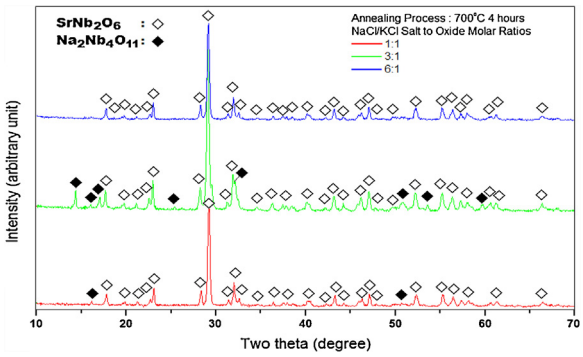

Fig. 1. XRD results of pure $SrNb_2O_6$ powders synthesized with different (1:1, 3:1, 6:1) salt to oxide molar ratios at 700 °C for 4 h.

and vacuum filtered several times to remove ionic salts from the oxides. The presence of the Cl^- ions in filtrate was checked by using qualitative reactions.

The surface morphology and microstructure of powders were examined by scanning electron microscopy (SEM; Jeol JSM 5910LV) equipped with EDS (Oxford Instruments Inca X-Sight 7274). X-ray diffraction patterns of powders were obtained using Rigaku Rotaflex model RU200B diffractometer using Cu Kα radiation (k = 1:546 Å) with a step size of 0.02° in the 2θ range of 15–60°. The average crystallite sizes of the powders were calculated using the Scherrer equation (1) [16]:

$$D = \frac{k \cdot \lambda}{B \cdot \cos\theta} \quad (1)$$

where D is a mean particle size (nm); k is a constant (taken as 0.9); λ = 0.15406, the wavelength of Cu Kα; B is the full width at half-maximum (rad); θ is the angle (°) between incident and diffracted beams.

Emission spectra of the powders doped with Nd^{3+} ions were measured in the wavelength-range of 1020–1120 nm and at the temperature of 300 K under 800 nm excitation from a diode laser (LDI-820). Fluorescence from the samples were focused on the slit of a Monochromator (Mc Pearson Model 2051) and detected by PMT (Hamamatsu 7102) detector. All of the photoluminescence measurements were performed at room temperature.

3. Results and discussions

3.1. X-ray diffraction analysis

Fig. 1 shows the XRD patterns that $SrNb_2O_6$ powders were synthesized by molten salt method using the salt/oxide molar ratio of 1:1, 3:1 and 6:1 at 700 °C for 4 h. Among the synthesized $SrNb_2O_6$ samples, the salt/oxide molar ratio of 6:1 was selected for the Nd^{3+} doped sample due to the single $SrNb_2O_6$ phase (JCPDS: 28-1243).

$SrNb_2O_6$ is formed at 700 °C by the reaction given as below:

$$2Sr(NO_3)_2 + 2Nb_2O_5 \rightarrow 2SrNb_2O_6 + 4NO + 3O_2$$

Fig. 2 shows the XRD patterns of pure, 0.5, 3 and 6 mol% Nd^{3+} doped $SrNb_2O_6$ powders synthesized by molten salt synthesis at 700 °C for 4 h. Synthesis of $SrNb_2O_6$ powders via molten salt route by using the salt/oxide molar ratio of 6:1 gave single phase $SrNb_2O_6$ (JCPDS: 28-1243). Also, it was observed a secondary phase $Na_2Nb_4O_{11}$ (JCPDS: 20-1145) at 6% doping concentration. In addition, trace of this unwanted crystalline phase is formed by the following reaction:

$$Na_2O + 2Nb_2O_5 \rightarrow Na_2Nb_4O_{11}$$

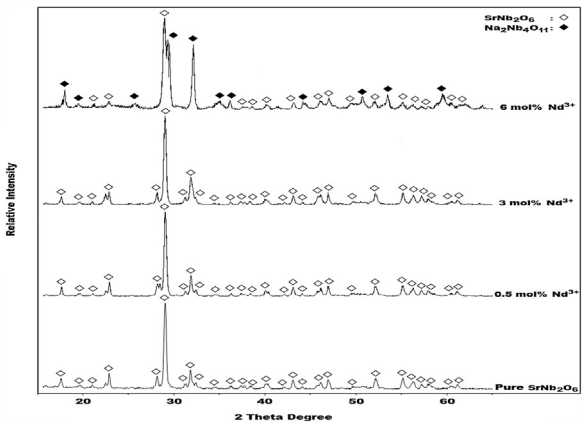

Fig. 2. XRD results of pure, 0.5, 3 and 6 mol% Nd^{3+} doped $SrNb_2O_6$ powders synthesized with 6:1 molar ratio at 700 °C for 4 h.

Table 1
Crystallography and refinement data for $SrNb_2O_6$.

Formula	$SrNb_2O_6$
Crystal system	Orthorhombic
Space group	*P21/c*
a (Å)	11.1272
b (Å)	7.7337
c (Å)	5.6265
V (Å^3)	484.19
Z	4
2θ range (deg.)	15–65
Step (°/min)	2
Program	MDI Jade 6.5

Table 2
Average crystallite size of $SrNb_2O_6$ and $SrNb_2O_6$:Nd^{3+} powders.

Nd^{3+} concentration (%)	Crystallite size (nm)
–	27.56
0.5	26.93
3	25.54
6	24.07

The volume fraction of $Na_2Nb_4O_{11}$ phase increases as compared to the volume fraction of $SrNb_2O_6$ phase with increasing dopant concentration. It is because of the fact that the activation energy for crystallization of minor phase $Na_2Nb_4O_{11}$ is higher than the activation energy of major phase [17].

XRD analysis indicated that powder samples crystallized in orthorhombic symmetry with space group *P21/c* having columbite structure. The lattice parameters of pure $SrNb_2O_6$ were calculated as a = 11.1272 Å, b = 7.7337 Å, c = 5.6265 Å and V = 484.19 Å^3 as shown in Table 1.

XRD revealed the average powder crystallite sizes along with doping concentration found by Scherrer's equation. While the crystallite size of undoped powder was 27.56 nm, it decreased with Nd^{3+} concentration and varied from 26.93 nm to 24.07 nm for doping levels of 0.5% and 6% respectively as shown in Table 2.

3.2. SEM-EDS analyses

SEM-EDS observations confirmed the XRD findings. The SEM micrographs of the pure $SrNb_2O_6$ and Nd^{3+} doped powders are illustrated in Fig. 3(a–d).

As it is seen from the SEM analysis, the grain shape of the $SrNb_2O_6$ phase exhibited varying morphology from rod to plate shape depending on Nd^{3+} doping concentration. The average grain size also decreased with the increasing Nd^{3+} content. While grain

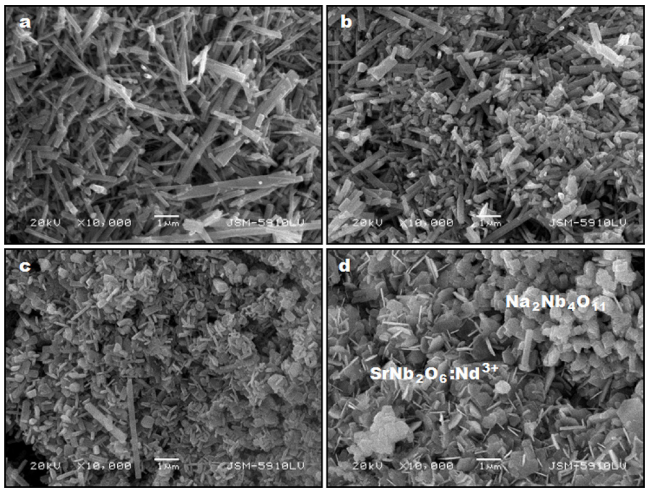

Fig. 3. Scanning electron microscopy (SEM) images of pure, 0.5, 3 and 6 mol% Nd^{3+} doped $SrNb_2O_6$ powders.

Table 3
Shape and grain size distribution with Nd^{3+} content.

Nd^{3+} conc. (mol%)	Phase	Grain shape	Grain size (μm)
–	$SrNb_2O_6$	Rod	Length 0.2–10 Thickness 0.07–0.6
0.5	$SrNb_2O_6$:Nd^{3+}	Round	Length 0.2–6 Thickness 0.07–0.4 0.1–1.0
3	$SrNb_2O_6$:Nd^{3+}	Round Plate	0.1–0.7 Size 0.2–2.0
6	$SrNb_2O_6$:Nd^{3+}	Plate	Size 0.2–1.0 Thickness 0.06–0.2
	$Na_2Nb_4O_{11}$	Round	0.4–1.5

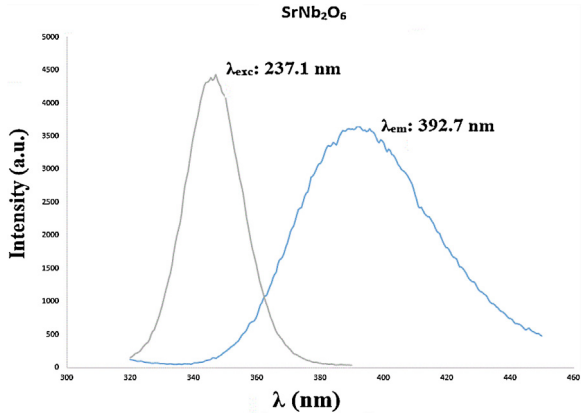

Fig. 4. Excitation and emission spectra of pure $SrNb_2O_6$ powders at 300 K.

size of the pure powder ranges between 0.2 and 10 μm length and 0.07–0.6 thickness, it was 0.2–1.0 μm size and 0.06–0.2 μm thickness for 6 mol% Nd^{3+} doping concentration, as shown in Table 3.

3.3. Optical measurements

Luminescence measurements measured upon 800 nm excitation contains two bands corresponding to the transitions from the $^4F_{3/2}$ to $^4I_{11/2}$ and $^4I_{9/2}$ levels. Emission spectra of the laser transition at 1062 nm due to the $^4F_{3/2} \rightarrow {}^4I_{11/2}$ transition measured at 300 K are shown in Fig. 4

As it can be seen from the emission spectra, it was found that the J-manifolds of Nd^{3+} ions were split due to symmetry of $SrNb_2O_6$ cation sites and the spectral profile and the number of the Stark

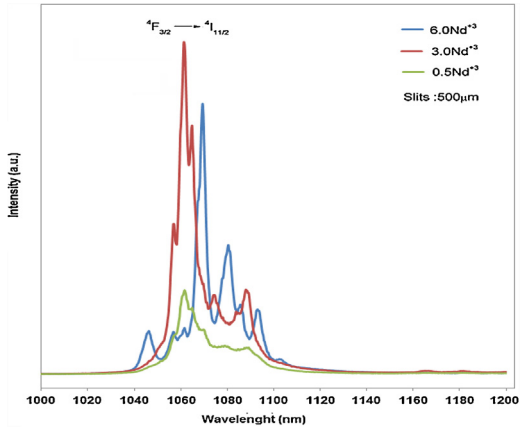

Fig. 5. Emission spectra of 0.5, 3 and 6 mol%:Nd^{3+} doped $SrNb_2O_6$ for the $^4F_{3/2} \rightarrow {}^4I_{11/2}$ transition in Nd^{3+} ions at 300 K.

components was the same for the 0.5 and 3 mol% Nd^{3+} doped powders. This behavior can be explained from the fact that the local symmetry of ligand ions surrounding of Nd^{3+} ions were same for the 0.5 and 3 mol% Nd^{3+} doped samples where the local symmetry of the ligand ions were different for 6 mol% Nd^{3+} doped sample in minor phase due to the crystallographical site change of Nd in $Na_2Nb_4O_{11}$ structure showing the slight difference on the emission spectra.

While the 0.5 and 3 mol% Nd^{3+} doped samples were calcined at elevated temperature, the $SrNb_2O_6$ crystals were becoming mature and Nd^{3+} ions were thermally diffused to the Sr^{2+} or Nb^{5+} positions in $SrNb_2O_6$ lattice as luminescent centers.

Considering the ionic ratios of Sr^{2+} (1.32 Å), Nb^{5+} (0.64 Å) and Nd^{3+} (1.123 Å) [18], location of the Nd^{3+} ions has been estimated as SrO_6 octahedral sites due to their similar ionic ratios except the different crystallographic site for the 6 mol% Nd^{3+} doped sample.

Because of cross-relaxation and non-radiative relaxation mechanism, it can also be seen from Fig. 4 that, concentration quenching occurred Nd^{3+} ions in the powder was 6.0 mol% of Nd^{3+} concentration. According to cross-relaxation mechanism, such neighbour Nd ions in the decreased ion spacing might transfer the energy each other and lead to the concentration quenching with increasing concentration of Nd ions.

In our study at 700 °C, the emission bands were observed at 1057–1088 nm for the 0.5, 3 mol% Nd doped samples and 1046–1101 nm for the 6 mol% Nd doped samples, respectively.

3.4. Laser induced emission spectra of $SrNb_2O_6$ powders

Luminescence measurements measured upon 805.2 nm excitation contains two bands corresponding to the transitions from the $^4F_{3/2}$ to $^4I_{11/2}$ level. Emission spectra of the laser transition at about 1060 nm due to the $^4F_{3/2} \rightarrow {}^4I_{11/2}$ measured at 300 K are shown in Fig. 5.

As it clearly can be seen from the emission spectra in Fig. 5, it was found that the J-manifolds of Nd^{3+} ions were split due to symmetry of $SrNb_2O_6$ cation sites and the spectral profile and stark level were the same for the two powders except for the 6 mol% due to high concentration of Nd^{3+}. This behaviour can be explained from the fact that the local symmetry of ligand ions surrounding of Nd^{3+} ions were same for 0.5 and 3 mol% powders. Concentration quenching occurred in the 6.0 mol% Nd^{3+} doped powder. This can be explained by cross-relaxation, if the positions of the Nd^{3+} ions are uncorrelated, the probability that an excited ion has another Nd^{3+} ion sufficiently nearby to cross-relax rapidly is proportional to the Nd^{3+} concentration. Thus, the linear relationship between

acceptor concentration and Nd^{3+} concentration is consistent with quenching by cross-relaxation. Interpreted quenching in terms of direct cross-relaxation between excited Nd^{3+} ions and randomly spaced unexcited ions.

4. Conclusion

Undoped and Nd-doped $SrNb_2O_6$ crystalline powders were successfully synthesized by molten salt synthesis method at a relatively low temperature than that of the other traditional conventional methods. The spectroscopic properties of the Nd^{3+} ions in $SrNb_2O_6$ single crystal are reported. XRD analysis showed that undoped and Nd^{3+} doped powders were single phase with orthorhombic structure with the *Pbcn* space group excluding the 6 mol% Nd doped sample. SEM and EDS results in accordance with those of XRD. The luminescence properties of the powders indicated that the concentration quenching occurs when the concentration of Nd^{3+} ions in the powder was 6.0 mol%.

Acknowledgment

This study was financially supported by the Marmara University Research Fund (BAPKO) with the project number FEN-A-150513-0171.

References

[1] J.H. Sturdivant, The crystal structure of columbite, Z. Kristallogr. 75 (1930) 88–105.
[2] M.K. Ekmekçi, M. Erdem, A. Mergen, G. Özen, B. Di Bartolo, Molten salt synthesis and spectral properties of Nd^{3+} doped $CdNb_2O_6$ columbite phosphors, J. Alloys Compd. 591 (2014) 230–233.
[3] Y. Zhou, M. Lü, Z. Qiu, A. Zhang, Q. Ma, H. Zhang, G. Zhou, Z. Yang, Photoluminescence characteristics of pure and Dy-doped $ZnNb_2O_6$ nanoparticles prepared by a combustion method, J. Phys. Chem. C 111 (2007) 10190–10193.
[4] R. Zhou, X. Wei, S. Huang, Y. Chen, M. Yin, Efficient near infrared quantum cutting in Yb^{3+} doped $CaNb_2O_6$ phosphor based on energy transfer, J. Alloys Compd. 537 (2012) 123–126.
[5] J. Cao, Y. Ji, J. Li, Z. Zhu, Y. Wang, Z. You, C. Tu, Crystal growth, Judd Ofelt analysis and fluorescence properties of Tm^{3+}:$CaNb_2O_6$ crystal, J. Lumin. 131 (2011) 1350–1354.
[6] D.A.S.S. Camargo, R.A. Silva, J.P. Andreeta, L.A.O. Nunes, Stimulated emission and excited state absorption in neodymium-doped $CaNb_2O_6$ single crystal fibers grown by LHPG technique, Appl. Phys. B 80 (2005) 497–502.
[7] D.A.S.S. Camargo, C.R. Ferrari, R.A. Silva, L.A.O. Nunes, A.C. Hernandes, J.P. Andreeta, Spectroscopic features of erbium-doped $CaNb_2O_6$ (M = Nb,Ta) single crystal fibers grown by laser heated pedestal growth technique, J. Lumin. 128 (2008) 223–226.
[8] D. Prabhakaran, F.R. Wondre, A.T. Boothroyd, Preparation of large single crystals of ANb_2O_6 (A = Ni, Co, Fe, Mn) by the floating-zone method, J. Cryst. Growth 250 (2003) 72–76.
[9] I.S. Mulla, N. Natarajan, A.B. Gaikwad, V. Samuel, U.N. Guptha, V. Ravi, A coprecipitation technique to prepare $CoTa_2O_6$ and $CoNb_2O_6$, Mater. Lett. 61 (2007) 2127–2129.
[10] N. Chaiyo, N. Vittayakorn, Effect of calcination conditions on phase formation of microwave dielectric cobalt niobate ($CoNb_2O_6$) powders via mixed oxide synthesis route, J. Ceram. Process. Res. 9 (4) (2008) 381–384.
[11] S. Kobayashi, S. Mitsuda, M. Ishikawa, K. Miyatani, K. Kohn, Anisotropic growth kinetics in the geometrically frustrated isosceles triangular Ising antiferromagnet $CoNb_2O_6$, Phys. Rev. B 60 (1999) 3331.
[12] M. Unruan, N. Vittayakorn, R. Wongmaneeruang, A. Prasatkhetragarn, S. Ananta, R. Yimnirun, Synthesis and properties of $Pb(Co_{1/3}Nb_{2/3})O_3$ ceramics, J. Alloys Compd. 466 (2008) 264–267.
[13] M. Maeda, T. Yamamura, T. Ikeda, Dielectric characteristics of several complex oxide ceramics at microwave frequencies, Jpn. J. Appl. Phys. Part 1 26 (Suppl. 2) (1987) S76–S79.
[14] A. Belous, O. Ovchar, B. Jancar, J. Bezjak, The effect of non-stoichiometry on the microstructure and microwave dielectric properties of the columbites $A^{2+}Nb_2O_6$, J. Eur. Ceram. Soc. 27 (2007) 2933–2936.
[15] A.G. Belous, O.V. Ovchar, A.V. Kramarenko, D.O. Mishchuk, B. Jancar, J. Bezjak, D. Suvorov, Effect of nonstoichiometry on the structure and microwave dielectric properties of cobalt metaniobate, Inorg. Mater. 42 (2006) 1369–1373.
[16] P.W.C. Sarvezuk, E.J. Kinast, C.V. Colin, M.A. Gusma, J.B.M. da Cunha, O. Isnard, J. Appl. Phys. 109 (2011), 07E160.
[17] A.G. Belous, O.V. Ovchar, A.V. Kramarenko, D.O. Mishchuk, B. Jancar, J. Bezjak, D. Suvorov, Effect of nonstoichiometry on the structure and microwave dielectric properties of cobalt metaniobate, Inorg. Mater. 42 (12) (2006) 1369–1373, 2006.
[18] K.H. Yoon, Y.S. Cho, D.H. Lee, D.H. Kang, Powder characteristics of $Pb(Mg_{1/3}Nb_{2/3})O_3$ prepared by molten salt synthesis, J. Am. Ceram. Soc. 76 (1993) 1373–1376.